Nanoscale Zero-Valent Iron Efficient for Remediation of Chromium, Nickel, and Cadmium-Contaminated Soils Near Oil Refinery Sites

Graphical abstract

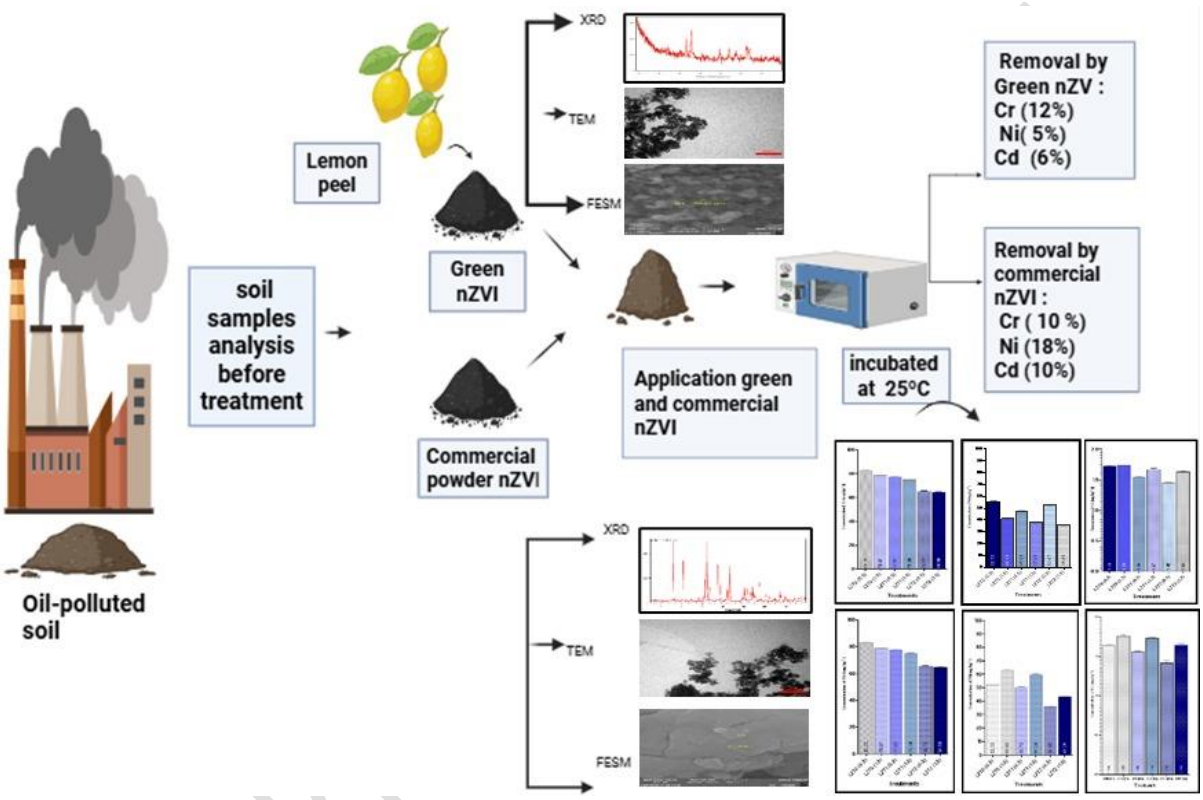

Nanoscale Zero-Valent Iron Efficient for Remediation of Chromium, Nickel, and Cadmium-Contaminated Soils Near Oil Refinery Sites

Shakar Jamal Aweez[1]*, and Ismaeel Tahir Ahmad [2]

[1]Department of Scientific Research Centre, Salahaddin University- Erbil, Erbil, Iraq; shakar.aweez@su.edu.krd

[2]Department of Soil and Water, College of Agriculture, Salahaddin University-Erbil, Erbil, Iraq. ismaeel.ahmad@su.edu.krd

*Correspondence: shakar.aweez@su.edu.krd

Abstract

Pollution of soil with heavy metals is a great environmental threat. This investigation soils affected by the refinery discharges of Gwer Road, Erbil, Iraq, focusing on physicochemical properties of soils, baseline contamination, and nanoscale zero-valent iron remediation. soil samples were taken from southern and northern 50m and 200m distances and 30cm depth. Soil texture, pH, and cation exchange capacity influenced the distribution of heavy metals. Chromium (52.85-79.54 $mg.kg^{-1}$), nickel (41.10-63.42 $mg.kg^{-1}$), and cadmium (1.41-1.76 $mg.kg^{-1}$) exceeded Environmental Baseline Standards (EBS), indicating refinery-derived pollution. The study evaluated the remediation potential of green-synthesized nanoscale-zero valent iron(nZVI) nanoparticles from lemon peel extract and commercial nZVI. Nanoparticle characterization using field-emission scanning electron microscopy (FESEM), transmission electron microscopy (TEM), and X-ray diffraction (XRD) techniques confirmed the nanoparticle size, core-shell shape, and crystallinity. Application of 0.5 g/kg

soil provided 12%, 5%, and 6% removal efficiencies for Cr, Ni, and Cd using green nZVI, compared to 10%, 18%, and 10% using commercial nZVI. Although green nZVI removes chromium similarly, it is sustainable, locally sourced, and cost-effective. Remediation efficacy was influenced by soil properties, baseline contamination, and nanoparticle characteristics. This study represents the first application of green and commercial nZVI for the remediation of refinery-affected soil, providing a sustainable approach for mitigating heavy metal pollution and enhancing industrial site management.

Keywords: Cadmium, Chromium; Heavy metals; Nickel, Nanoscale zero-valent iron, Oil-refinery impacted soil; Remediation

1. Introduction

Oil is a contemporary necessity for humanity. However, as oil production rises, the oil industry is becoming one of the most environmentally disastrous enterprises, due to oil extraction, refining, distribution, and storage. The oil industry's environmental impacts include substantial atmospheric pollution emissions, woodland loss, the exclusion of significant land areas from economic use, disruption to the geological integrity of aquifers, and the contamination of surfaces and groundwater by oil products. (Strizhenok and Ivanov, 2021). Leakage of crude oil and refined products from pipes, storage tanks, and transportation apparatus further contributes to environmental degradation. Soil quality and fertility are affected by leakage of crude oil as well as processed products, causing soil to become contaminated. (Khalefah et al., 2024)

Industrial effluents discharges, and refinery byproducts cause the accumulation of heavy metals into the soil and water systems (Francy *et al*., 2020; Al-Khafaji and Kareem, 2021). Discharges from refineries comprise total petroleum hydrocarbons (TPH) and heavy metals, which include chromium, vanadium, zinc, iron, nickel, and copper. Additional toxic

pollutants present include oil, grease, phenols, ammonia, sulphides, suspended solids, nitrogen compounds, and cyanides. Heavy metal-contaminated soil is particularly destructive to the soil because it alters physical and chemical properties, and fertility and ecological balance (Mirza and Ahmed, 2023; Kareem and Abdulla, 2023; Xu et al., 2025). The residue of oil refineries contains harmful substances, including lead, cadmium, and mercury, which are important contributors to heavy metal pollution in the environment and neighboring areas. (Samaila et al., 2022)

Carbon nanotubes and nanoscale zero-valent iron (nZVI) nanoparticles are commonly used to remediate oil and organic pollutant-contaminated soils. Adsorption and catalytic degradation make them effective. When employed with surfactant foams, nZVI degrades DDT and PCB particularly well. Nanoparticle characteristics, surfactant content, and soil physicochemical qualities all affect metal removal effectiveness and must be improved.(Vu andMulligan,2023).The nanoscale dimension of these materials results in a large surface area to volume ratio, providing numerous reactive sites that enhance their interaction with environmental contaminants (Aydogan et al., 2022). Nanoparticles are defined as a distinct physical, chemical, and biological property that has a size of 1-100 nm and also comes with a surface charge and quantum effects. These characteristics have led to the fact that nanomaterials have become the most effective and promising agents when it comes to the treatment of heavy metals in polluted soils. (Narkhede et al.,2024). High surface reactivity, many active sites, and eco-friendliness make nZVI useful for immobilizing and removing heavy metals from environmental matrices. (Mousa et al., 2024).

Soils surrounding the refinery exhibited localized heavy metal contamination, especially chromium (Cr), nickel (Ni), and cadmium (Cd), exceeding Environmental Baseline Standards (EBS). Contamination patterns varied with distance, direction, and soil texture, highlighting the influence of environmental factors on metal distribution. the contamination

variance indicates the role of distributional environmental factors. Despite well-documented refinery-related pollution at this site, no studies have evaluated nanomaterial-based remediation in these soils, creating a critical knowledge gap. This study investigates the remediation efficiency of green-synthesized nanoscale zero-valent iron (nZVI) synthesized using lemon peel extract, which served as a natural reducing and capping agent, compared with commercial nZVI for the removal of Cr, Ni, and Cd from refinery-contaminated soils along Gwer Road, Erbil, Iraq. This study presents a cost-effective and eco-friendly nanomaterial synthesized from plant-derived residues and represents the first site-specific comparative application of green and commercial nZVI in a refinery-affected soil site, providing a sustainable framework for heavy metal remediation and providing both scientific and practical significance for environmental management.

2. Materials and Methods

2.1 Soil Sampling

Soil samples were collected in April 2024 near oil refineries along Gwer Road, roughly 15 kilometers from Erbil city. Samples were taken from two locations and two different distances (0.5 and 1.5 m) with an auger at a depth of 30 cm. This covered area is affected by refinery residues (see Table 1and Figure 1). The samples were placed in labeled plastic bags and transported to the laboratory for analysis.

Table 1. GPS reading of the study sites.

Site	Latitude N	Longitude E
Site 1(50m)	36° 8'32.01"	43°46'32.84"
Site 1(200m)	36° 8'30.95"	43°46'30.93"
Site2(50m)	36° 8'30.97"	43°46'29.07"
Site2(200m)	36° 8'28.88"	43°46'25.09"

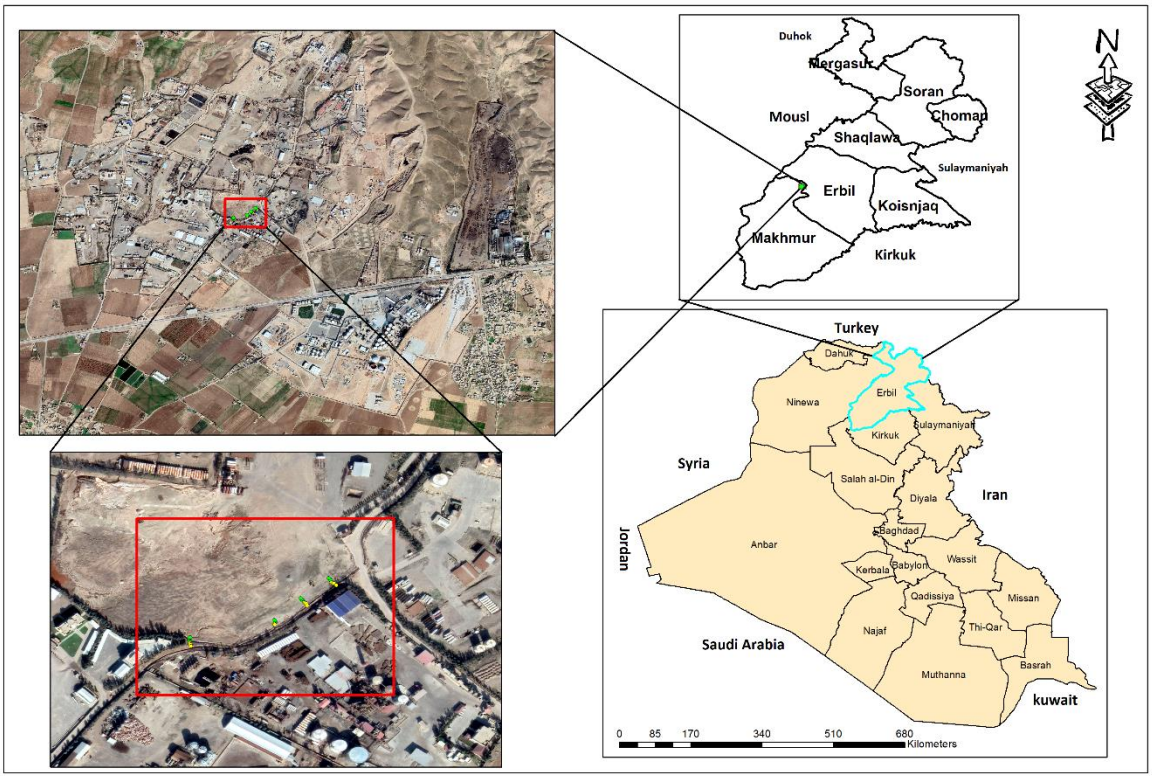

Figure 1. The geographical location of the study area of polluted soils, as shown from a satellite image

2.2 Soil Characterization

The soil samples were air-dried at room temperature for 72 hours, then gently crushed with a wooden rod, and sieved through a 2 mm mesh to remove any coarse fragments. Soil physicochemical properties were determined with standard procedures. Soil pH was measured using a HANNA pH meter (EDGE) in a 1:2.5 soil to water suspension. Organic matter content was estimated using the Walkley–Black method. Soil particle size distribution was determined using a hydrometer, and cation exchange capacity was determined using the ammonium acetate (NH_4OAc) method. Heavy metals (Cr, Ni, Cd) total concentrations in both treated and untreated soils were determined using X-ray fluorescence (XRF Rigaku NEX CG). All analyses were performed in triplicate, and to ensure precision and

consistency, the quality control included procedural blanks, duplicates, and standard reference materials. (Aweez et al., 2021; Mirza and Ahmed, 2023; Kareem and Abdulla, 2023).

2.3 Green Zero valent iron nZVI Materials

2.3.1 Plant Material and Extract

Lemon peel (*Citrus Limonium*) biomass was harvested in Alwa, Erbil city. The samples were rinsed with distilled water, dried in an oven at 70 °C for 48 hours, and crushed to a fine powder. The powder was refined using double-distilled water, dried at 65 °C, and stored at 4 °C until required. To obtain the extract, 100 g of the powder was combined with 1000 mL of distilled water. The mixture was boiled for 5 minutes, left to cool, and then filtered three times using Whatman No. 1 paper to obtain a clear aqueous extract the method described by (Madivoli et al., 2019; Sun et al., 2022).

2.3.2 Synthesis of Green Zero-Valent Iron Nanoparticles

Green nZVI was produced by mixing equal quantities of 0.1 M $FeCl_3 \cdot 6H_2O$ solution and lemon peel extract, with continuous vortexing for 3 minutes at room temperature. The formation of nZVI was signified by a color transition from yellow to black. The nanoparticles were separated using centrifugation at 6000 rpm, rinsed with a 1:1 ethanol-water solution, and subsequently dried at 60 °C (Madivoli et al., 2019; Sun et al., 2022). Figure 2 shows the synthesis process.

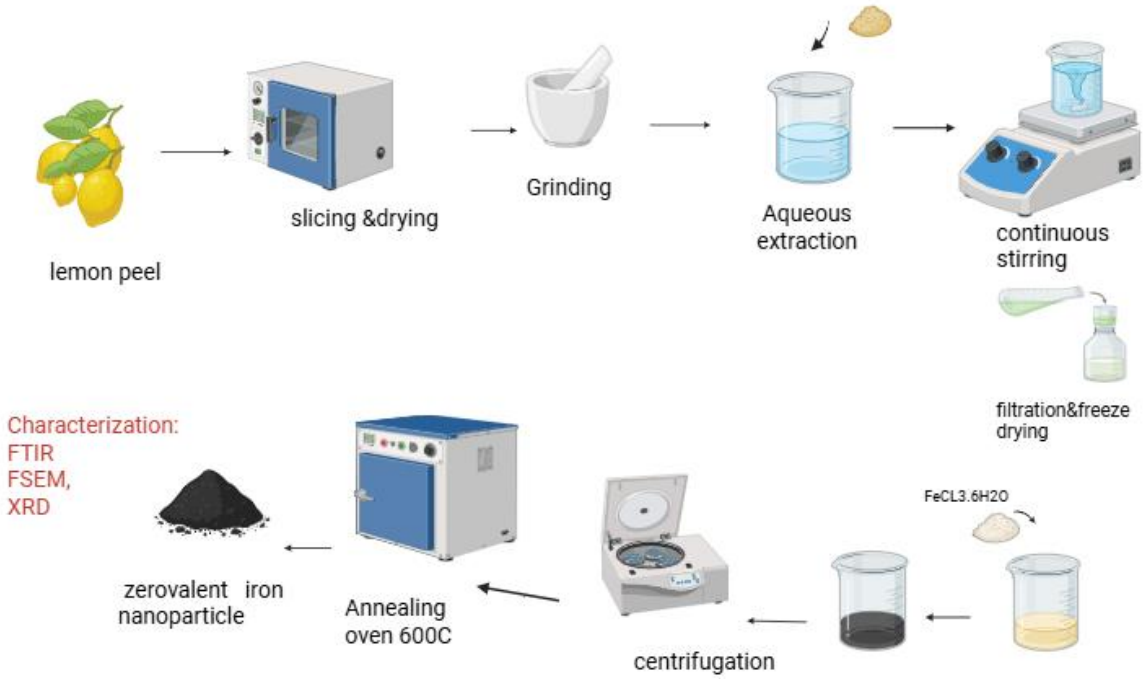

Figure 2. Synthesis of green Zero-Valent iron nanoparticles (nZVI)

2.3.3 Characterization of nanoscale zero-valent iron (nZVI)

The morphology, size, and crystallinity of nZVI were analyzed using FESEM, TEM, and XRD techniques. FESEM revealed mainly spherical particles with a uniform distribution, TEM showed the interior structure and nanoscale features, while XRD confirmed a metallic Fe^0 core, which is essential for enhanced reactivity (Madivoli *et al.,* 2019; Sun *et al*., 2022).

2.4 Nano-Remediation Experiment

To experiment, 100 grams of soil were mixed with either 0.5 grams of green nZVI or commercial nZVI. Seven milliliters of distilled water were then added to achieve a moisture content of 7.9%. The mixtures were then incubated at 25 °C for seven days to promote metal reduction (Felix *et al*., 2018; Sun *et al*., 2022; Abdullah and Darwesh, 2023).

2.5 Contaminant Removal Rate

153 The percentage removal rate of contamination serves to distinguish the volume of eliminated
154 contaminants by comparing the initial and final heavy metal concentrations in treated soil.
155 (Francy *et al.,* 2020).
156 $R = (Ci - Cf) / Ci * 100$
157 Where:
158 R signifies the removal rate (%)
159 Ci defines the original contamination concentration,
160 Cf represents the final contamination concentration.
161 2.6 Data Analysis
162 All analyses were performed in triplicate, and results were expressed as mean ± standard
163 deviation. Statistical comparisons were conducted using one-way ANOVA, and significant
164 differences between means were considered at $p \leq 0.05$. And graph pad Prism is used for
165 graph production. (Karim and Goran,2023; Mirza and Ahmed, 2023)

166 **3. Results**

167 3.1 Physicochemical properties of the soils according to distances (50m and 200m), and
168 directions (south and north) from the oil refinery

169 Table 2 indicates that the physicochemical characteristics and heavy metal concentrations of
170 soils collected at two distances (50 m and 200 m) and in two directions (south and north)
171 relative to the refinery. Soil texture varied with proximity at 50 m, soils were predominantly
172 sandy clay loam (SCL) and clay loam (CL), whereas at 200 m, sandy loam (SL) textures
173 dominated, indicating a gradual increase in coarser fractions with distance from the source
174 of contamination. Soil pH values ranged from 6.25 ± 0.05 to 7.93 ± 0.04, showing slightly
175 acidic to neutral conditions near the refinery (50 m) and nearly neutral to weakly alkaline
176 conditions farther away (200 m). Northern samples generally exhibited slightly higher pH

than southern ones. The cation exchange capacity (CEC) ranged from 20.25 ± 0.35 to 83.23 ± 0.80 cmolc.kg^{-1} with the highest values recorded in northern soils at 200 m. Lower CEC values in southern soils at 50 m.

Table 2. Physicochemical properties of the soils according to distances (50m and 200m), and directions (south and north) from the oil refinery (CL: clay loam, SCL: silty clay loam, SL: silty loam)

Soil Characteristics	Sample point	Distance	South	North
Soil texture	50	0.5	SCL	SCL
		1.5	SCL	CL
	200	0.5	SCL	SL
		1.5	SCL	SL
pH	50	0.5	7.13±0.05	7.22±0.03
		1.5	6.25±0.05	7.23±0.02
	200	0.5	7.93±0.04	7.92±0.03
		1.5	7.56±0.05	7.82±0.04
Cation Exchange Capacity	50	0.5	33.33±0.50	20.33±0.3
(CEC)cmol(c).kg^{-1}		1.5	25.54±0.40	20.25±0.3
	200	0.5	44.65±0.60	60.34±0.7
		1.5	23.07±0.45	83.23±0.8
		1.5	52.85±0.80	54.32±1.2

185 3.2 Heavy metal concentration of the soils according to distances (50m and 200m), and
186 directions (south and north) from the oil refinery

187 Table 3 presents the concentrations of chromium (Cr), nickel (Ni), and cadmium (Cd) in
188 soils collected at two distances (50 m and 200 m) and two directions (south and north) from
189 the refinery. Heavy metal concentrations varied spatially, reflecting the influence of both
190 distance and wind dispersion patterns. Chromium (Cr) concentrations ranged from 52.85 ±
191 0.80 to 83.23 ± 3.29 mg. kg^{-1}, nickel (Ni) from 41.10 ± 0.83 to 63.42 ± 1.65 mg. kg^{-1}, and
192 cadmium (Cd) from 1.41 ± 0.03 to 1.76 ± 0.03 mg. kg^{-1}. The highest Cr and Ni values were
193 recorded in soils located 50 m from the refinery, particularly at northern sampling points,
194 whereas concentrations declined noticeably at 200 m. In contrast, Cd concentrations showed
195 minimal variation with distance and direction, suggesting a more uniform distribution of this
196 metal within the study area.

197 **Table 3.** Heavy metal Concentration depending on the distances (50m and 200m) and
198 directions (south and north) of the oil refinery

Sample Point	Distance	Direction(m)	Cr(mg.kg^{-1})	Ni (mg.kg^{-1})	Cd(mg.kg^{-1})
50	0.5	South	79.54±0.37	55.69±1.49	1.73±0.08
50	1.5	North	83.23±3.29	52.33±0.80	1.64±0.02
50	0.5	South	63.45±0.62	41.10±0.83	1.74±0.05
50	1.5	North	78.79±1.29	63.42±1.65	1.76±0.03
200	0.5	South	63.41±1.00	42.95±0.77	1.41±0.03
200	1.5	North	56.12±1.10	46.17±0.11	1.53±0.03
200	0.5	South	52.85±0.80	45.09±0.87	1.47±0.06

200	1.5	North	54.32±1.21	45.51±1.07	1.46±0.02
Environmental Bassline Stander (EBS) Hama & Darwesh (2019)			23	34	1.10

199 3.2 Characterization of nZVI Particles

200 FESEM analysis Figure 3 is a representation of the FESEM images of the nanoparticles.
201 Figure 3(a) shows that the average diameter of particles is about 46.27nm, which shows a
202 uniform dispersion, and consistent shape. Conversely Figure 3(b)shows larger particles with
203 an average size of about 55.97 nm, characterized by a stratified or plate-shaped morphology
204 and smaller nanoparticles and smaller nanoparticle on the surface. The morphologies of the
205 two types of nZVI synthesized in green were mostly spherical and the average diameter of
206 the green nZVI was 26 nm, which indicate the difference in sizes and shapes between the
207 two green and commercial of nanoparticles.

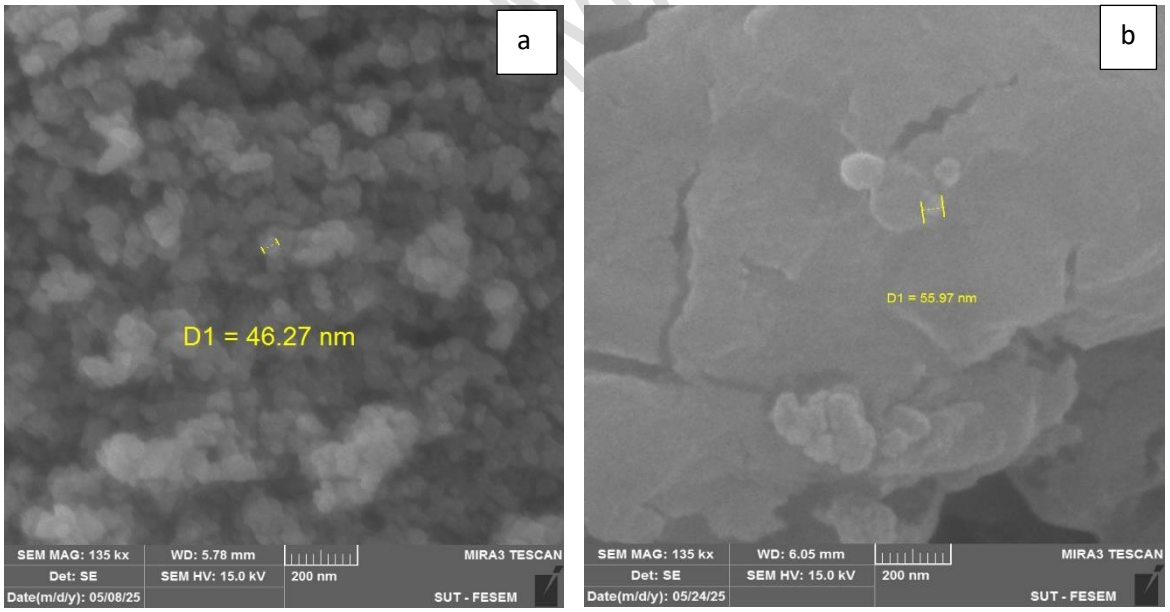

209 **Figure 3.** FESEM images of nanoscale zero valent-iron (nZVI) particles: (a) from green
210 nanoparticle; (b) commercial nanoparticle.

211

TEM analysis

Figures 4(a) and 4(b) are TEM images that show aggregates of black nanoparticles at different geometries with diverse sizes. The main aggregates of the particles exhibit an average size of approximately 100 nm. It can be observed that there is a considerable degree of aggregation, which might be attributed to the high surface energy of the nanoparticles, leading to clustering of the nanoparticles during the sample preparation. Subsequent analysis by TEM shows that the nanoparticles have densely packed atomic structures, meaning that they are either crystalline or semicrystalline, and they are probably made of metals or metal oxides.

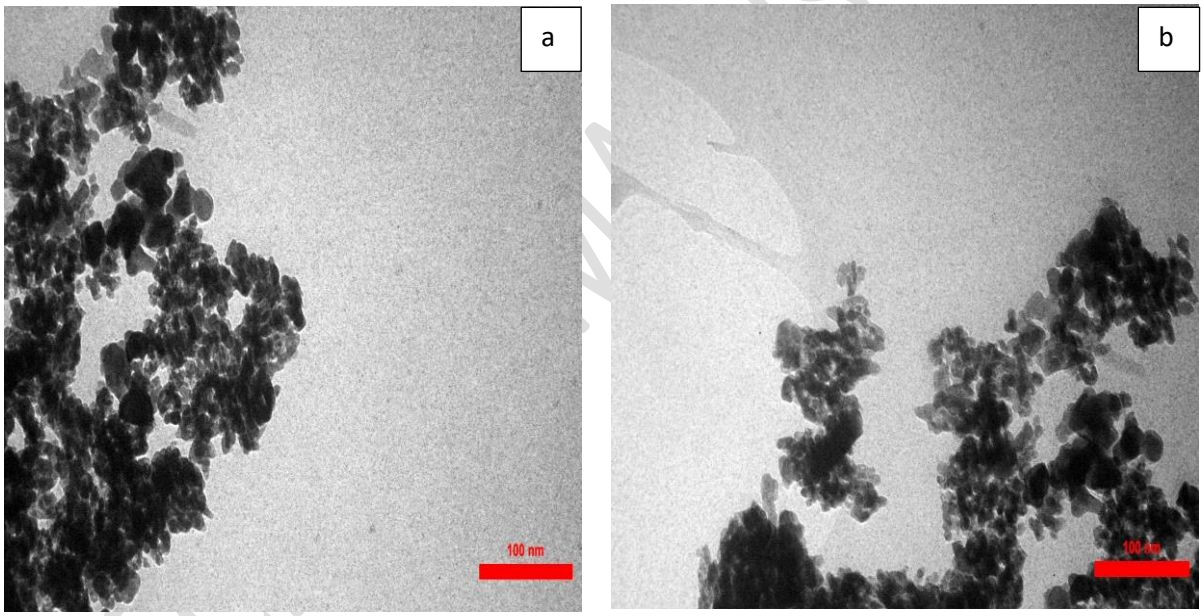

Figure 4. TEM image of nanoscale zero-valent iron (nZVI)particles (a)from green nanoparticles ;(b) Commercial nanoparticles.

XRD analysis

Figure 5 illustrates the X-ray diffraction (XRD) patterns of the produced nanoparticles. Figure 5(a) displays a combination of broad and sharp peaks, with a prominent peak at $2\theta = 25°$, demonstrating the existence of nanocrystalline domains and indicating a largely amorphous character along with reduced particle size. Additional peaks at about $2\theta = 30°$,

35°, and 40° are associated with distinct crystallographic planes. Conversely, Figure 5(b) displays distinct, sharp diffraction peaks at 2θ angles of 15°, 22°, 33°, and 36°, which correspond to the (111), (200), and (220) planes of cubic structures. These observations collectively confirm the crystalline structure of the nanomaterials.

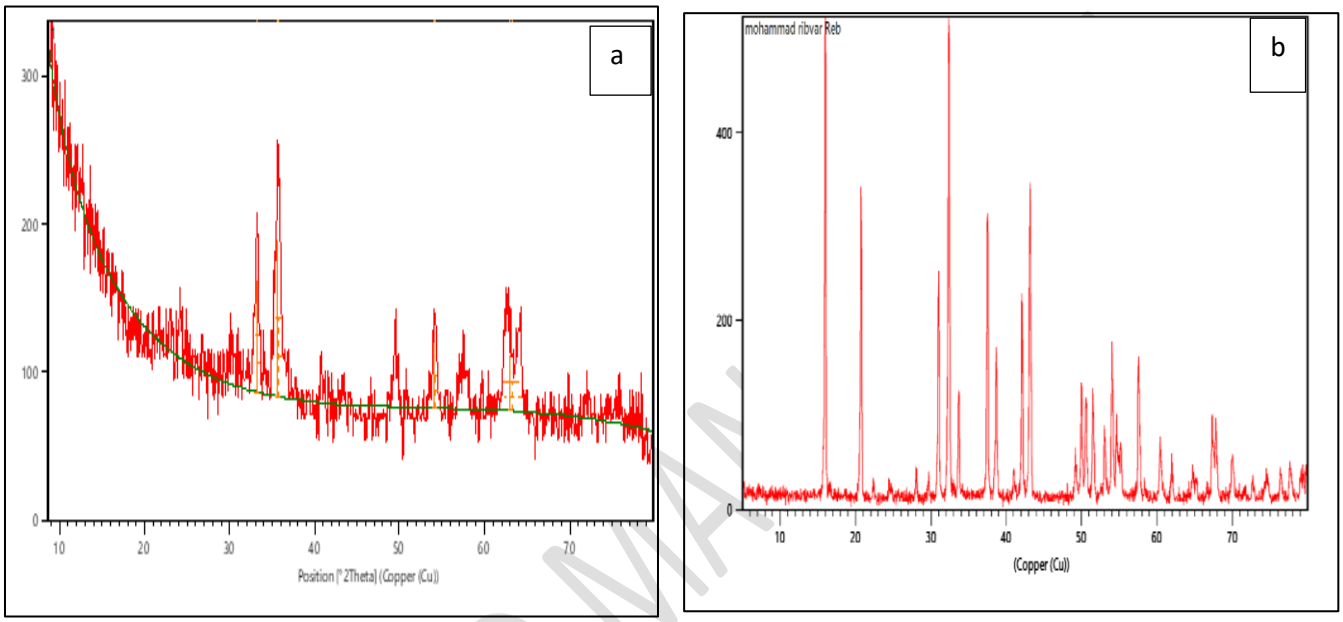

Figure 5.XRD image of nanoscale zero-valent iron(nZVI)particles:(a) green nanoparticles;(b) commercial nanoparticles.

3.3 Remediation of polluted soil

3.3.1. Remediation of Chromium (Cr)concentration in the crude oil stream's surrounding soils at different distances from two different locations

Figures 6 (a & b) illustrate the chromium (Cr) contents in soils sampled at varying distances from two areas affected by crude oil. Data analysis demonstrated that the utilization of nZVI significantly ($p \leq 0.05$) effects chromium concentrations in the contaminated soils. The maximum chromium concentrations were measured at 79.53, 64.42, 83.23, and 55.8 $mg.kg^{-1}$ at sample locations S1L1D1T0, S1L2D1T0, S2L1D1T0, and S2L2D1T0, respectively. The minimum concentrations recorded were 46.25, 43.35, 64.49,

and 52.92 mg.kg^{-1} at S1L1D2T1, S1L2D2T2, and S2L1D2T2, respectively. These results indicate a consistent north to south variation in Cr reduction subsequent nZVI treatment.

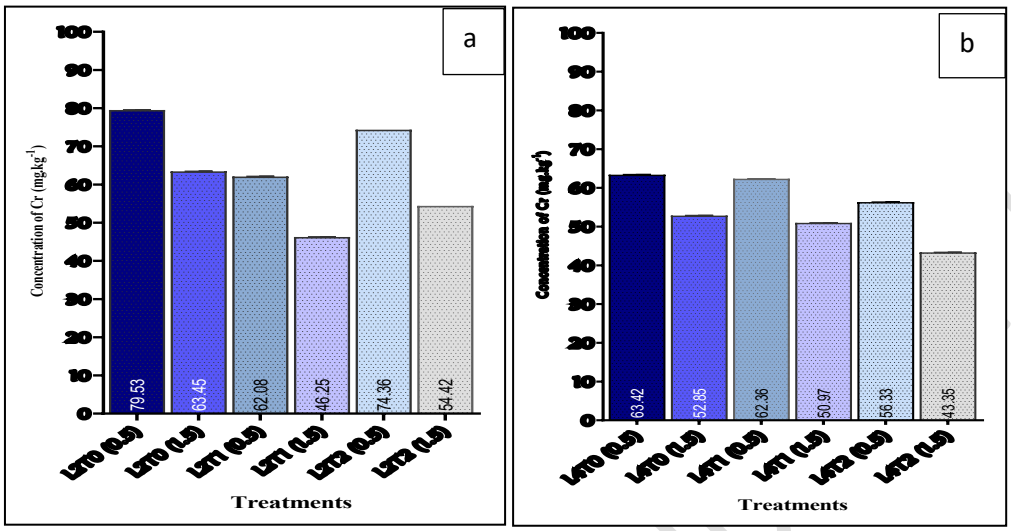

Figures 6. (a &b) Remediation of contaminated soil using green and chemically synthesized nZVI particles (dosage: 0.5 g/kg of soil): (a) Cr concentration L2(50m) from source; (b) Cr concentration L4 (200m) from source, south location. distance (0.5), (1.5), T0: without treatment, T1: green nanoparticle treatment, T2: commercial nanoparticle treatment.

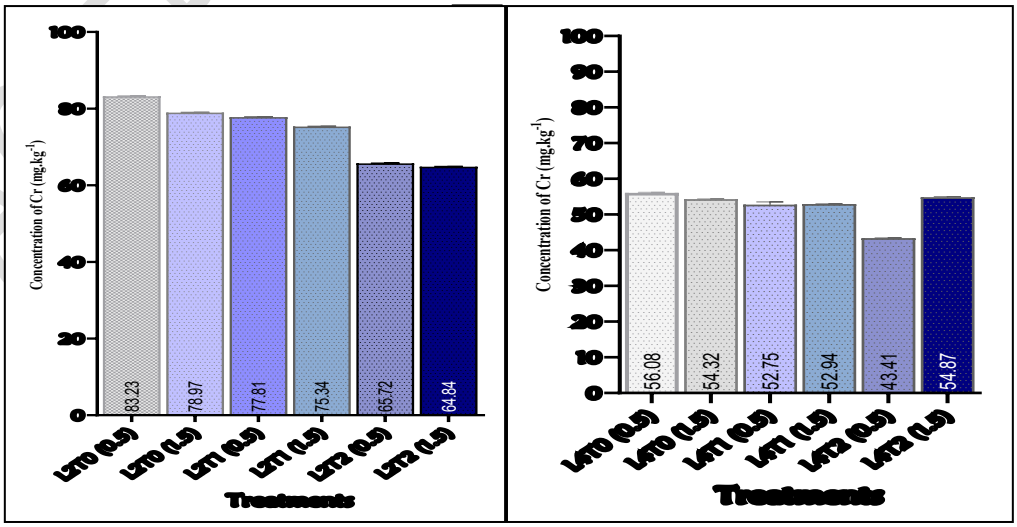

Figures 6. (a &b) Remediation of polluted soil utilized green and commercial synthesize n ZVI particles (dosage:0.5g/kg of soil) :(a) Cr concentration L2 (50m) from source; (b) Cr

concentration from source L4 (200m), north location, distance (0.5), (1.5), T0: without treatment, T1: green nanoparticle treatment, T2: commercial nanoparticle treatment.

3.3.2. Remediation of Nickel (Ni) content in the crude oil stream's surrounding soils at different distances from two different directions

Figures 7 (a & b) illustrate the nickel (Ni) concentrations in soils sampled at varying distances from two crude oil-contaminated sites. Data analysis demonstrated that the utilization of nZVI considerably ($p \leq 0.05$) decreased Ni concentrations in contaminated soils. The maximum nickel concentrations were 55.69, 45.09, 63.42, and 45.87 $mg.kg^{-1}$ at sample locations S1L1D1T0, S1L2D2T0, S2L1D2T0, and S2L2D1T0, respectively. The minimum concentrations were 35.84, 34.45, 35.86, and 40.61 $mg.kg^{-1}$ at S1L1D2T2, S1L2D2T2, S2L1D1T2, and S2L2D2T1, respectively. These results indicate a consistent north-to-south variation in Ni reduction following nZVI treatment.

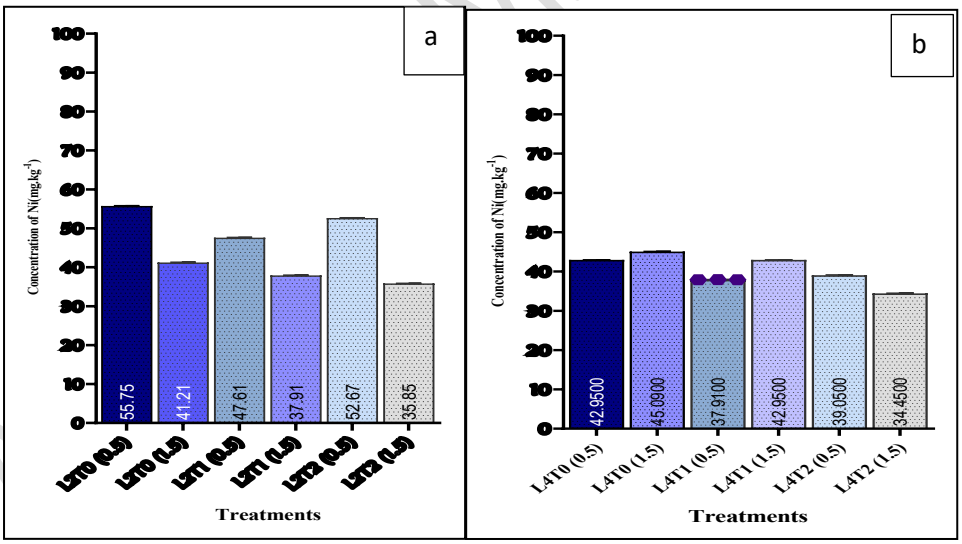

Figures 7 (a&b) Remediation of contaminated soil utilized Green and commercial synthesized n ZVI particles (dosage:0.5 g/kg of soil) :(a) Ni concentration L2 (50m) from source ;(b) Ni concentration L4(200m) from source, south location distance T0: without treatment, T1: green nanoparticle treatment, T2: commercial nanoparticle treatment.

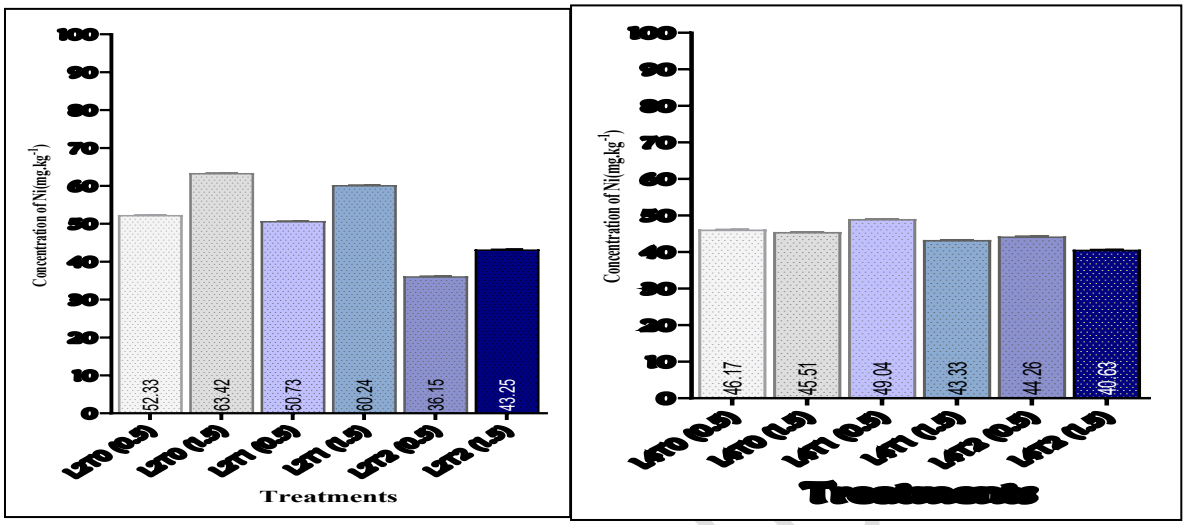

Figures 7. (a&b) Remediation of polluted soil utilizes green and commercial synthesized nZVI particles (dosage:0.5 g/kg of soil): (a)Ni concentration L2 (50m) from source ;(b) Ni concentration L4 (200m) from source, north location. Distance (0.5), (1.5), T0: without treatment, T1: green nanoparticles, T2: commercial nanoparticles treatment.

3.3.3 Remediation of cadmium (Cd) content in the crude oil stream's surrounding soils at different distances from two different directions

Figures 8. (a & b) illustrate the cadmium contents in soils sampled at varying distances from two areas affected by crude oil. Data analysis demonstrated that the utilization of nZVI markedly ($p < 0.05$) diminished Cd concentrations in contaminated soils. The maximum Cd concentrations recorded were 1.73, 1.47, 1.76, and 1.53 mg/kg at S1L1D1T0, S1L2D2T0, S2L1D2T0, and S2L2D1T0, respectively. The minimum values recorded were 1.44, 1.23, 1.41, and 1.41 $mg.kg^{-1}$ at S1L1D1T2, S1L2D1T2, S2L1D1T2, and S2L2D2T1, respectively.

The results demonstrate a consistent north-south variation in nickel reduction following to nZVI treatment.

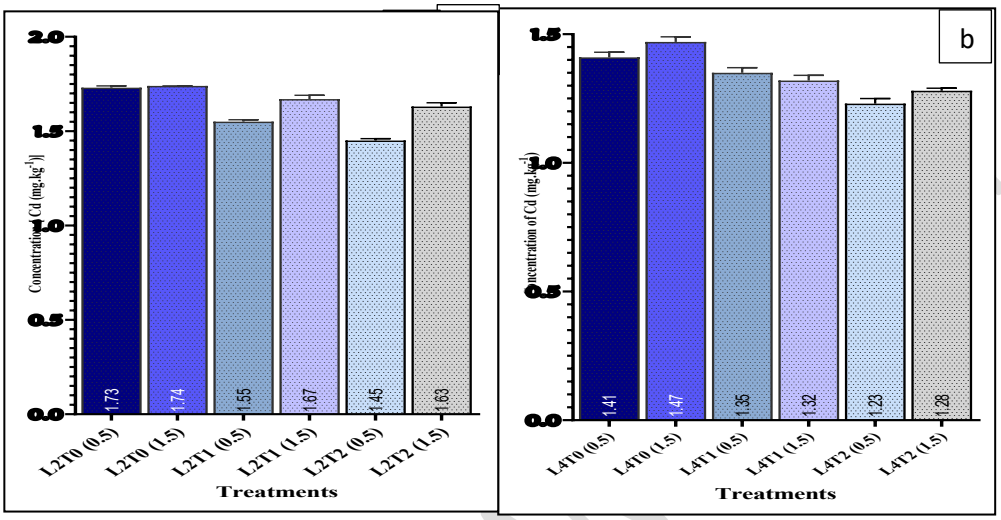

Figures 8. (a&b). Remediation of polluted soil utilize green and commercial synthesized n ZVI particles (dosage:0.5g/kg of soil) :(a) Cd concentration from location L2 (50m); (b) Cd concentration from location L4 (200m) from south location distance (0.5), (1.5), T0: without treatment, T1: green nanoparticle treatment, T2: commercial nanoparticle treatment.

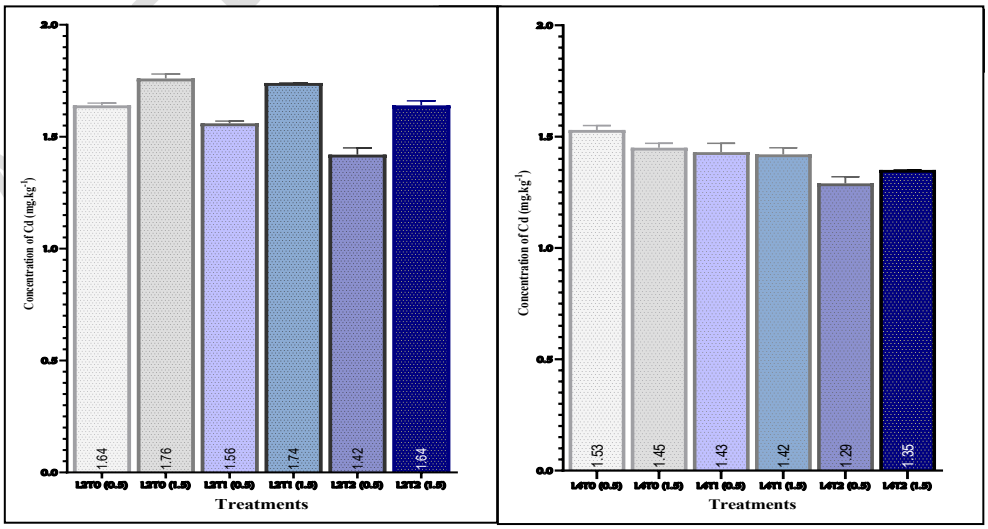

Figures 8. (a&b). Remediation of polluted soil utilized green and commercial n ZVI particles (dosage:0.5g/kg of soil) :(a) Cd concentration at distance(50m) ;(b) Cd concentration at distance(200m) from the north location, T0: without treatment, T1: green nanoparticle treatment, T2: commercial nanoparticle treatment.

3.4 Efficiency Removal Rate

Table 4 illustrates the efficacy of heavy metal removal utilizing both green and commercial nanoparticles. The higher removal efficiencies recorded were (27%, 21%, 15%, 33%, 10%, and 17%) at sample locations (S1P1D2T1, S2P1D1T2, S1P1D1T1, S2P1D2T1, S1P1D1T1, and S1P1D1T2,) respectively. The lower removal efficiencies recorded were (3%, 4%, 1%, 4%, 2%, and 4%) at (S2P2D2T1, S2P2D2T2, S2P2D1T1, S2P2D1T2, S2P1D2T1, and S2P2D2T2) respectively. Green-synthesized nZVI achieved average removal efficiencies of (12%, 5%, and 6%) for Cr, Ni, and Cd, respectively, whereas commercial nZVI obtained (10%, 18%, and 10%) for the same metals. Efficiency removal rate of both green(T1) and commercial (T2) n ZVI treatments significantly reduced concentration of Cr, Ni, and Cd in oil-polluted soils (Table 3). Green nZVI showed similar Cr removal to commercial nZVI, while commercial nZVI achieved higher reductions for Ni and Cd.

Table 3. The efficiency of nZVI particles in removing heavy metals from oil-polluted soils

			Removal Efficiency of Nanoparticles (RE)					
Location	**Sample point**	**Distances**	**Cr Green %**	**Cr Commercial %**	**Ni Green %**	**Ni Commercial %**	**Cd Green %**	**Cd Commercial nZVI**

S1	P1(50)	D1(0.5)	22%	7 %	6 %	15 %	10 %	17 %
		D2(1.5)	27%	14 %	12 %	8 %	4 %	6 %
	P2(200)	D1(0.5)	15%	6 %	1 %	12 %	4 %	12 %
		D2(1.5)	8%	9 %	4 %	18 %	10 %	13 %
S2	P1(50)	D1(0.5)	7%	21 %	3 %	32 %	5 %	14 %
		D2(1.5)	5%	18 %	5 %	33 %	2 %	8 %
	P2(200)	D1(0.5)	6%	4 %	1 %	7 %	6 %	9 %
		D2(1.5)	3 %	4 %	4 %	16 %	3 %	4 %
Average Removal efficiency			12%	10%	5%	18%	6%	10%

4. Discussion

4.1. Physicochemical properties

Soils revealed clear spatial variation in relation to the refinery.

Soils at 50 m soils shows pH value of 6.25-7.23, which is a sign of slightly acidic to neutral environment. This could be as a result of petroleum residues which is credible considering that soil pH is reduced because organic acid is formed as a result of breaking hydrocarbons. In comparison, Soil at 200 m exhibited higher pH values (7.567.93) and these are nearer to the neutral level and slightly alkaline (7.93) implying a reduced effect by the refinery emissions. There is great variability in the cation exchange capacity (CEC). The values of CEC of the soils in the south at 50m, 20.25 to 83.23 cmolc.kg $^{-1}$, are rather low and this is probably caused by the decomposition of organic matter as well as the effects of contamination on clay and organic matter. Comparatively, the soils in the north with 200 m distance from source have a greater CEC of 83.23 cmolc.kg $^{-1}$ because they have a fine texture with a smaller pollutant load, which increases exchange capacity because of the low content of clay. The results indicate that the soil texture clay loam (CL) and sandy clay loam (SCL) at 50 m contained more metals and had less variation in CEC, whereas sandy loam

(SL) at 200 m allowed the movement and exchange of ions. These findings agree with those that indicating that contamination of petroleum hydrocarbons decreases the pH level and increases the electrical conductivity of the soil. (Sharma and Vashishtha,2021; Ogbeide and Eriyamremu,2023).

4.2. Morphological and Structural Characterization of nZVI

FESEM images (Figure 3a, b) demonstrate the differences in particle sizes and morphologies between the green-synthesized and commercial nZVI. The nZVI generated by the 'green synthesis' process and stabilized by phytochemicals from plant extracts predominantly included spherical nanoparticles, with an average size of 26 nm. The biomolecules, polyphenols, and flavonoids were also useful as natural reducing and capping agents, which controlled the nucleation and growth of Fe 0 nanoparticles and prevented aggregation. Commercial nZVI, by contrast, had larger particles, 46 -56 nm, with irregularly layered or plate-like morphologies, which do not imply the presence of organic stabilizers, and imply that growth and aggregation of particles is unimpeded. The FESEM results were confirmed with TEM analysis (Figure 4a, b), which showed black nanoparticle aggregates of irregular shapes with mean cluster sizes of about 100 nm. The size aggregates of dimension were likely to be generated during the drying and preparation of the sample, by surface energy, through magnetic interactions, and by aggregation of smaller particles. The TEM/FESEM analysis quantitative analysis of the images (n=100) showed that the particles had an average size of 25.9 ± 13.0 nm (D_{50} = 25 nm), indicating there is reasonable homogeneity in size. The XRD technique has been used to establish the crystalline nature of the two variations of nZVI (Figure 5a, b). The synthesised nZVI exhibited with green methods was relatively broader and had less strong diffraction peaks with a pronounced peak at 2 θ = 25 ^{o}, which corresponded to amorphous nanocrystalline domains of smaller crystallite sizes. Supplementary peaks were observed at 30°, 35°, and 40°, indicating partial oxidation to Fe

400 $_3$ O $_4$. Commercial nZVI exhibited stronger and pronounced peaks at 15°, 22°, 33°, and 36°,
401 which is consistent with (111), (200), and (220) planes of body-centered cubic Fe^0, which
402 means that there is an improvement of crystallinity and crystallite size. The crystallite size,
403 determined through the Scherrer equation (K = 0.9, 1.5406 Å), was approximately 22 nm of
404 the green-synthesized nZVI, which is closely related to the TEM analysis, meaning that most
405 of the particles were single-crystalline. while zeta potential and surface area of the BET
406 analysis were not conducted in the present research, the results of the FESEM, TEM, and
407 XRD revealed that the nZVI particles possess a diminutive particle size, a spherical shape,
408 and crystalline Fe^0 phases, which have been confirmed to increase the heavy-metal
409 adsorption and reduction. Both nZVI commercially available and green-synthesized have
410 surface and structural properties that indicate the aspects of successful remediation, which
411 involve the reduction of Cr, Ni, and Cd in soils that have been polluted. The studies reveal
412 that the synthesis procedure, type of plant extract employed, and the solvent environment
413 have a pronounced effect on the particle size, morphology, and stability, and consequently,
414 they corroborate the current findings. (Boonruam et al., 2020; Abdelfatah et al., 2021;
415 Aydogan et al., 2022; Apriliani, 2022 Elizondo-Villarreal et al., 2022).

416 4.3. Heavy Metal Concentrations

417 The soils located near the refinery exhibited unique but localized patterns of contamination,
418 which were also adjusted by the changes in the spatial distance, directions, and soil textures.
419 The peak concentrations of Cr (52.85–79.54 $mg.kg^{-1}$) and Ni (41.10–63.42 $mg.kg^{-1}$) were
420 seen at a distance of 50 m from the refinery, but Cd (1.41–1.76 $mg.kg^{-1}$) exhibited relatively
421 lower levels. All observed amounts of heavy metals in this study exceeded the
422 Environmental Baseline Standards (EBS) established by Hama and Darwesh (2019) (Cr: 23
423 $mg.kg^{-1}$, Ni: 34 $mg.kg^{-1}$, Cd: 1.1 $mg.kg^{-1}$), indicating significant pollution from refinery

activities. After the treatment, nanoscale zero-valent iron (nZVI) was effective in reducing the level of heavy metals in all sites. The chromium (Cr) concentration decreased to 43.35mg.kg-1. This corresponds to the whole conversion in the hexavalent chromium (Cr^{6+}) into the trivalent chromium (Cr^{3+}) through reactive elemental iron (Fe^{0}). Nickel (Ni) and Cadmium (Cd) were reduced to 34.45mg. kg^{-1} and 1.23mg. kg^{-1} respectively, likely due to the high adsorption rates to the high surface area of nZVI particles. The great reductions were found near the source of contamination, which showing the effect of the nature of soil, such as the concentration of organic matter, the texture of the soil, and the pH on the nZVI reactivity and the speciation of metals. The reduced Ni and Cd removal efficiency of nZVI green-synthesized compared with commercial nZVI is likely due to the phytochemical capping layer added in the green synthesis. The stability of nanoparticles is increased in this organic coating, but it is also known to decrease the availability of active sites on the surface that can be adsorbed or reduced by the metal. This phytochemical capping coating improvable nanoparticle stability and limits aggregation, but it partially prevents the accessibility of reactive Fe^{0} sites. This leads to the reduction of electron transfer and surface adsorption reactions, especially with divalent metal ions, like Ni^{2+} and Cd^{2+}. In contrast, commercially used nZVI does not have organic capping compounds and therefore presents a larger fraction of Fe surfaces and increases its abilities to take part in redox reactions and metal adsorption. The carboxyl, hydroxyl, and carboxyl groups found as part of the plant-derived coating can potentially have a preferential interaction with the species of chromium, thus further decreasing the active sites of Ni^{2+} and Cd^{2+}. This selective binding, in combination with steric hindrance caused by the capping layer, lowers the efficiency of the metal removal in systems using green-synthesised nZVI. These findings are consistent with the other research that indicates that green-synthesised nZVI is capable of reducing the levels of Cr and Ni, as well as adsorbing Cd in soils affected by the refinery

process, and performance is strongly dependent on soil pH, texture, and the level of organic matter (González-Feijoo et al., 2023). Moreover, variations in plant extract compositions during the synthesis may affect the particle size, the surface area, and surface chemistry, thus changing the selectivity of metal binding (Ali et al., 2023).

4.4. Efficiency Removal Rate

The redox potential of hexavalent chromium (Cr^{6+}) is very large and thus, its reduction to trivalent chromium (Cr^{3+}) occurs rapidly. In contrast, nickel (II) (Ni^{2+}) and cadmium(II) (Cd^{2+}) are removed largely through the adsorption process since their reduction is unlikely within these conditions, both elements rather react with the iron oxide and hydroxide layers that grow over the surface of nano-particles of zero-valence iron (nZVI) during production. A phytochemical capping layer of a green-synthesized nZVI is based on plant extracts, which increases the colloidal stability but partially covers the Fe^{0} sites. This limits direct Fe^{0} interactions and electron transfer, reducing the number of available sites for Ni^{2+} and Cd^{2+} adsorption. Commercial nZVI, which possesses little to no surface capping, exposes more Fe 0 sites and, therefore, shows better removal efficiency toward the two metals. Mechanically, the increased removal efficiency of nickel (Ni) compared with cadmium (Cd) may be attributed to the fact that Ni has a smaller ionic radius and is more attracted to the surfaces of iron hydroxide/oxides, which enhances adsorption. The characteristics of soils, such as pH, cation exchange capacity, and the amount of organic matter, also promote Ni binding more than Cd, therefore, thus impacting the differences in the removal efficiency. These findings are consistent with the recent studies that demonstrate green synthetic nanoparticles often show reduced removal of Ni and Cd than chemically synthesized zero-valent iron nanoparticles (nZVI), which is mostly explained by the different surface coating and reactivity (Abdullah and Darwesh, 2023; Francy et al., 2020)

5. **Conclusion**

- The soils near the refinery contained high levels of contamination of chromium (52.8579.54 mg.kg^{-1}), nickel (41.1063 mg.kg^{-1}63), and cadmium (1.41-1.76mg.kg-^{1}), all of which exceed the Environmental Basic Standards (EBS). The extent of contamination differed depending on the distance to the refinery, the soil texture, and the direction of sampling.
- Both green-synthesized and commercially obtained nanoscale zero-valent iron (nZVI) were effective in lowering concentrations of heavy metals in the contaminated soil.
- Green-synthesized nZVI exhibited comparable chromium removal efficiency to commercial nZVI, while reducin12% of chromium, a nickel removal efficiency of 5%, and a cadmium removal efficiency of 6%.
- Commercial nZVI eliminated 10 % chromium, 18 % nickel, and 10 % cadmium, and it has better capacity with nickel and cadmium due to the presence of a larger number of exposed Fe ^{0} reacting sites.
- A more sustainable and economical solution is provided with nZVI that is green-synthesized by utilizing plant-based materials that naturally possess stabilizing qualities, whereas the particles are small, morphologically spherical, and contain large Fe ^{0} cores, which are all essential to enable high reactivity.
- Soil characteristics, especially the soil texture, pH, and organic matter, are also very critical in the nanoparticle performance; therefore, site-specific tests in remediation processes are essential.

Future work

- For incubation, consider a duration of four weeks and evaluate is to be taken where doses greater than (0.5 g kg^{-1} of the soil) will be measured. The experiments should be done in the field in varying soil moisture and atmospheric conditions.
- To enable elimination of the heavy metal concentrations, the characterization of the surfaces of the nanoparticles, such as determining the zeta potential and surface area through the BET, is considered necessary to explain their stability, surface charge, and surface area.
- To improve the stability, reactivity, and scalability of green zero-valent iron nanoparticles, alternative plant extracts such as *Punica granatum* and organic amendments are to be used.

Acknowledgments: I would like to express my gratitude to my supervisor, Professor Ismail Ahmad Tahir, for his invaluable direction, guidance, and thorough supervision during the research period. I am also grateful for the technical support and supply of necessary laboratory facilities to Salahaddin University -Erbil, Erbil, Iraq.

Abbreviations:

Zero valent Iron Nanoparticle	nZVI
Transmission Electron Microscope	TEM
Field Emission Scanning Electron Microscopy	FESEM
X-ray Diffraction	XRD
Heavy Metals	HMs
Removal efficiency	RE

522 Soil, Point, Distance, Treatment SPDT

523 **Author Contributions**: Shakar Jamal Aweez is the conceptual and design author of the
524 study, the performer of the experimental processes, the data analysis, and the drafting author
525 of the original manuscript. Ismaeel Tahir Ahmad monitored and supervised the author and
526 further participated in the evaluation and improvement of the study.

527 **Financing:** This research was not externally financed.

528 **Data Availability Statement:** The datasets created and processed in the present study can
529 be provided by the respective author in accordance with a reasonable request.

530 **Conflicts of Interest:** The authors declare no conflicts of interest.

531 **Ethical approval**: This study was purely laboratory-based and involved the use of green
532 and commercial nanoparticles to remediate heavy metal-contaminated soil (oil) and did not
533 involve any human or live animal subjects.

534 **References**

535 Abdullah, Z. & Darwesh, D. A.(2023). Application of nanotechnology for remediation drill
536 cutting soil. *Zanco Journal of Pure and Applied Sciences,* **35,** 121-128.

537 Abdelfatah, A.M., Fawzy, M., Eltaweil, A.S. & El-Khouly, M.E. (2021). Green synthesis of
538 nano-zero-valent iron using *Ricinus communis* seeds extract: Characterization and
539 application in the treatment of methylene blue-polluted water. *ACS Omega*, **6**(39), 25397–
540 25411.

541 AL-Khafaji, B.Y., Kareem, N.Q. (2021). Impact of oil waste discharge from Al-Nassiriya
542 oil refinery upon physical-chemical properties and heavy elements content of vicinity soil.
543 *Univ. Thi-Qar J. Sci.* **8**(2), 11-15. https://doi.org/10.32792/utq/utjsci.v8i2.806

544 Al-Obaidy, A.H.M.J. & Shaia, H. (2019). Assessment of oil-polluted soil properties in Thi-
545 Qar Governorate, Iraq. *J. Univ. ThiQar Sci.*, 5(2), 23–31.

546 Ali, S., Zahid, A. & Shahid, S.T. (2023). Green engineering of iron and iron oxides by
547 different plant extracts. In: *Iron Ores and Iron Oxides – New Perspectives*. In tech Open
548 Apriliani, N. (2022). Green synthesis of nanoscale zero-valent iron and its activity as an
549 adsorbent for Ni (II) and Cr (VI). *Chemistry and Materials,* **1,** 71-76
550 Aweez, S. J., Darwesh, D. and Othman, B. (2021). Application of some single and integrated
551 index equation to assess heavy metal in different soils in Erbil Governorate. *Iraq J. Agric.*
552 *Sci.*, **52**, 868–875

553 Aydogan, T., Dumanlı, F. T. Ş. & Derun, E. M. (2022). Effect of lemon peel extract
554 concentration on nano-scale Fe/Fe3O4 synthesis. *Politeknik Dergisi,* **25,** 1423-1427.
555 Boonruam, P., Soisuwan, S., Wattanachai, P., Morillas, H. & Upasen, S. (2020). Solvent
556 Effect on Zero-Valent Iron Nanoparticles (nZVI) Preparation and Its Thermal Oxidation
557 Characteristic. *ASEAN Engineering Journal,* **10**.
558 Elizondo-Villarreal, N., Verástegui-Domínguez, L., Rodríguez-Batista, R., Gándara-
559 Martínez, E., Alcorta-García, A., Martínez-Delgado, D., Rodríguez-Castellanos, E. A.,
560 Vázquez-Rodríguez, F. & Gómez-Rodríguez, C. (2022). Green synthesis of magnetic
561 nanoparticles of iron oxide using aqueous extracts of lemon peel waste and its application in
562 anti-corrosive coatings. *Materials,* **15,** 8328.
563 Felix, O., Nwaogazie, I. L., Akaranta, O. & Abu, G. O. (2018). Removal of heavy metals in
564 spent synthetic-based drilling mud using nano zero-valent iron (nZVI). *J Sci Res Rep***, 1**-11.
565 Francy, N., Shanthakumar, S., Chiampo, F., & Sekhar, Y. R. (2020). Remediation of lead
566 and nickel contaminated soil using nanoscale zero-valent iron (nZVI) particles synthesized
567 using green leaves: First results. *Processes, 8*(11), 1453. https://doi.org/10.3390/pr8111453
568 González-Feijoo, R., Rodríguez-Seijo, A., Fernández-Calviño, D., Arias-Estévez, M. &
569 Arenas-Lago, D.(2023). Use of three different nanoparticles to reduce Cd availability in
570 soils: effects on germination and early growth of Sinapis alba L. *Plants,* **12,** 801.

571 Hama,R.H., and Darwesh,.D.A.(2O19).Heavy metals evaluation in soil of agricultural field
572 around a pond of gas plant in the kurdistan Region of iraq.ZANCO Journal of Pure and
573 Applied Science,**31**(5),28-35.
574 Kareem, K. K. H. & Abdulla, S. S. (2023). Determination of heavy metals and total
575 petroleum hydrocarbons in soil samples and plant leaves around oil refineries located on
576 erbil-gwer road. *Science Journal of University of Zakho,* **11,** 492-498.
577 Khalefah O., Omran A., Al-Waily M. (2024). An investigation on the environmental impact
578 of petroleum refinery effluent on soil pollution. *Int. J. Environ. Impacts*, 7(1), 45-58.
579 Madivoli, E. S., Kareru, P. G., Maina, E. G., Nyabola, A. O., Wanakai, S. I. & Nyang'au, J.
580 O. (2019). Biosynthesis of iron nanoparticles using *Ageratum conyzoides* extracts, their
581 antimicrobial and photocatalytic activity. *SN Applied Sciences,* **1,** 1-11.
582 Mirza, D. K. & Ahmed, I. T. (2023). Impact of crude oil discharge fromoil refineries near
583 gwer road of erbil city on soil physico-chemical Properties and Metal Emancipations.
584 *ZANCO Journal of Pure and Applied Sciences,* **35,** 78-87.
585 Mousa, M.A., AL-Farraj, A.S.F., AL-Wabel, M.I., Ibrahim, Usman, ARA., AL-Swadi, H.A.,
586 Ahmad, M., Rafique, M.I.(2024).The influence of nZVI composites as immobilizing agents
587 on the bioavailability of heavy metals and plant growth in mining-contaminated soil.Global
588 NEST journal,**26**(2),1-12
589 Narkhede, S., Parkhey, P., Dadsena, A., Singhai, A., Phillips, E., Kolla, V. & Sahu, R.(2024).
590 Green Synthesis of Silver Nanoparticles for Arsenic (III) Removal from Contaminated
591 Water.
592 Ogbeide, G.E. & Eriyamremu, G.E. (2023). Physicochemical and microbial alterations in
593 crude oil-contaminated soil samples. *Dutse Journal of Pure and Applied Sciences*, **9**(2a),
594 281–289. https://doi.org/10.4314/dujopas.v9i2a.28

595 Samaila B., Kalgo Z., Maidamma B. (2023). Exposure to heavy metals in oil and gas wastes:
596 A systematic review on health hazards assessment and mitigation in Nigeria." *Adv. Res. Med.*
597 *Health Sci.* **1**(1):22-32

598 Sappa, G., Barbieri, M., Viotti, P., Tatti, F. & Andrei, F. (2022). Assessment of zerovalent
599 iron nanoparticle (nZVI) efficiency for remediation of arsenic-contaminated groundwater:
600 two laboratory experiments. *Water,* **14,** 3261.

601 Strizhenok, A. V. & Ivanov, A. V. (2021). Monitoring of air pollution in the area affected
602 by the storage of primary oil refining waste. *Journal of Ecological Engineering,* ***22*****,** 60-67.
603 Sun, J., Luo, Y., Ye, J., Li, C. & Shi, J. (2022). Chromium distribution, leachability, and
604 speciation in a chrome plating site. *Processes,* **10,** 142.

605 Vu, K. A. and Mulligan, C. N. (2023). An overview of the treatment of oil pollutants in soil
606 using synthetic and biological surfactant foam and nanoparticles. *Int. J. Mol. Sci.*, **24**, 1916.
607 https://doi.org/10.3390/ijms24031916

608 Xu, X., Ren, J., Wang, N., Huiling, D.and Zeng, M.(2025).Study on the remediation effect
609 of biochar on heavy metals in coal gangue-contaminated soil. *Global NEST J.*, **27**(9).
610 https://doi.org/10.30955/gnj.07696